Infrared-active excitations related to Ho^{3+} ligand-field splitting at the commensurate-incommensurate magnetic phase transition in $HoMn_2O_5$

A. A. Sirenko,* S. M. O'Malley, and K. H. Ahn
Department of Physics, New Jersey Institute of Technology, Newark, New Jersey 07102, USA

S. Park
Rutgers Center for Emergent Materials and Department of Physics and Astronomy, Rutgers University, Piscataway, New Jersey 08854, USA

G. L. Carr
National Synchrotron Light Source, Brookhaven National Laboratory, Upton, New York 11973, USA

S-W. Cheong
Rutgers Center for Emergent Materials and Department of Physics and Astronomy, Rutgers University, Piscataway, New Jersey 08854, USA

(Received 29 March 2007; revised manuscript received 29 May 2008; published 6 November 2008)

Linearly polarized spectra of far-infrared (IR) transmission in $HoMn_2O_5$ multiferroic single crystals have been studied in the frequency range between 8.5 and 105 cm^{-1} and for temperatures between 5 and 300 K. Polarization of IR-active excitations depends on the crystallographic directions in $HoMn_2O_5$ and is sensitive to the magnetic phase transitions. We attribute some of the infrared-active excitations to electric-dipole transitions between ligand-field (LF) split states of Ho^{3+} ions. For light polarization along crystalline *b* axis, the oscillator strength of electric dipoles at low frequencies (10.5, 13, and 18 cm^{-1}) changes significantly at the commensurate-incommensurate antiferromagnetic phase transition at $T_3=19$ K. This effect shows a strong correlation with the pronounced steps of the *b*-directional static dielectric function. We propose that the LF on Ho^{3+} connects the magnetism and dielectric properties of this compound through coupling with the Mn spin structure. We comment on the possibility for composite excitations of magnons and excited LF states.

DOI: 10.1103/PhysRevB.78.174405 PACS number(s): 75.80.+q, 75.30.Ds, 75.47.Lx, 78.30.−j

I. INTRODUCTION

Interplay between the long-range magnetic and ferroelectric orderings has recently motivated extensive studies of rare-earth multiferroic manganites RMn_2O_5 (R=Tb, Dy, and Ho).[1–3] These materials are attractive for both fundamental studies and for possible device applications due to the intriguing phase diagram and magnetic-field-induced spontaneous electric polarization. A number of phase transitions occur at low temperatures. Upon cooling, Mn spins order in the *a*-*b* plane at $T_1 \approx 40-43$ K, and incommensurate (IC) order of Mn spins switches to commensurate (C) one at $T_2 \approx 37-39$ K and back to incommensurate order again at $T_3 \approx 15-25$ K. Finally, rare-earth spins order at lower temperatures below $T_4 \leq 10$ K. Anomalies in the dielectric constant and thermal expansion at T_1, T_2, T_3, and T_4, as well as appearance of spontaneous polarization along *b* axis at T_C, which coincides in $HoMn_2O_5$ with T_2, reflect changes in ferroelectric order and provide evidence for strong spin-lattice coupling in RMn_2O_5 multiferroics.[4]

Recent optical studies of spin-lattice dynamics in multiferroics progressed in several directions: conventional Raman-scattering spectroscopy of optical phonons[5,6] and infrared (IR) spectroscopy of the phonons,[7] as well as the low-frequency excitations called "electromagnons."[8–10] The report by Mihailova *et al.*[5] on the absence of optical phonon anomalies at the phase transitions in RMn_2O_5 (Ho, Tb) was followed by the observation of a very small (<1 cm^{-1}) anomalous shifts of the high-frequency optical phonons around T_1 in R=Bi, Eu, and Dy compounds.[6] While spectra of the Raman-active optical phonons demonstrate only minute variations, IR-active excitations in $RMnO_3$ (R=Gd and Tb) (Ref. 7) and $TbMn_2O_5$ (Refs. 8 and 10) show intriguingly strong changes at the phase-transition temperatures.

In this paper we present a systematic study of the far-IR transmission spectra in $HoMn_2O_5$ at low temperatures in the vicinity of the phase transitions using synchrotron-radiation-based Fourier-transform infrared (FTIR) spectroscopy. We report strong changes in the oscillator strength for low-frequency IR excitations measured for light polarization along different crystalline axes at the magnetic commensurate-incommensurate transition $T_3=19$ K. Weaker changes in the IR-excitation spectra at around $T_1=44$ K were followed by a slow decrease in absorption in the temperature range that is much higher than T_1 up to about 200 K. We explain the observed IR excitations at 10.5, 13, and 18 cm^{-1} as electric-dipole transitions between ligand-field (LF) states of Ho^{3+} ions. The change in the oscillator strength for low-energy IR excitations at T_3 is associated with modification of the wave-function symmetry for the

Ho^{3+} LF states, which is influenced by magnetic ordering of the Mn spin system.

II. EXPERIMENT

The high-temperature flux growth technique was utilized to produce bulk crystals of $HoMn_2O_5$ (see Ref. 1 for details). Samples with thickness of about 0.5 mm were oriented using x-ray diffraction. The opposite sides were polished and wedged with an ~7° offset in order to suppress interference fringes. Transmission intensity was measured at the U12IR beamline at the National Synchrotron Light Source at Brookhaven National Laboratory equipped with an Oxford optical cryostat, Bruker 125HR spectrometer, LHe-pumped (~1.4 K) bolometer, and two grid polarizers for incident and transmitted radiations, respectively. The frequency resolution of 0.6 cm^{-1} was chosen to be about three times smaller than the typical width of the absorption lines. The transmission intensity was measured with the incident beam perpendicular to the sample plane in various polarization configurations $z(x,y)$, where z stays for the direction of the light propagation and x and y denote electric polarization of incident and transmitted light, respectively. For each sample the raw data of transmitted intensity were normalized to transmission through an empty aperture with a size close to that of the sample.

Figure 1 shows transmission spectra of $HoMn_2O_5$ measured in $a(b,b)$, $b(a,a)$, and $a(c,c)$ configurations at $T=5$ K, which are dominated by absorption lines at 10.5, 13, 18, 37, 42, 52, and 97 cm^{-1}. Fast fringes between 60 and 90 cm^{-1} are due to the Fabry-Perot interference in the sample. A couple of additional higher-frequency absorption lines at 31 and 85 cm^{-1} appear in the spectra at higher temperatures, and their oscillator strengths increases quasilinearly with temperature up to about $T=60$ K. Transmission intensity maps (Fig. 2) were measured in $a(b,b)$, $b(a,a)$, and $a(c,c)$ configurations with the temperature increments of 0.5 K in the range of $T<50$ K and about 5 K at $T>50$ K. Drastic increase in absorption at 10.5, 13, 18, and 42 cm^{-1} occurs upon cooling at $T_3=19$ K for the $a(b,b)$ configuration, where electric field $\vec{e}$ of both incoming and transmitted light is parallel to the direction of spontaneous electric polarization along b axis.

Comparison of the temperature-frequency maps measured for several different $z(x,y)$ configurations demonstrated a relatively weak dependence on the direction of the light propagation direction z, as what is expected for oscillators with the $\vec{k}$ vector ≈0. At the same time, absorption spectra of anisotropic $HoMn_2O_5$ crystals depend strongly on the light *polarization* with respect to the crystallographic directions, in particular, whether we have the electric field of light perpendicular or parallel to the Mn spin ordering plane: $\vec{e} \| c$ and $\vec{e} \perp c$, respectively. For example, in the $a(c,c)$ transmission configuration the doublet at 10.5 and 13 cm^{-1} dominates the low-frequency part of the spectrum [see Fig. 2(b)]. Close to the temperature interval between $T_2=39$ K and $T_1=43$ K, this doublet merges to a single line with a frequency of about 12 cm^{-1}, which maintains a significant oscillator strength further above $T_1=43$ K, and it can be seen even at T

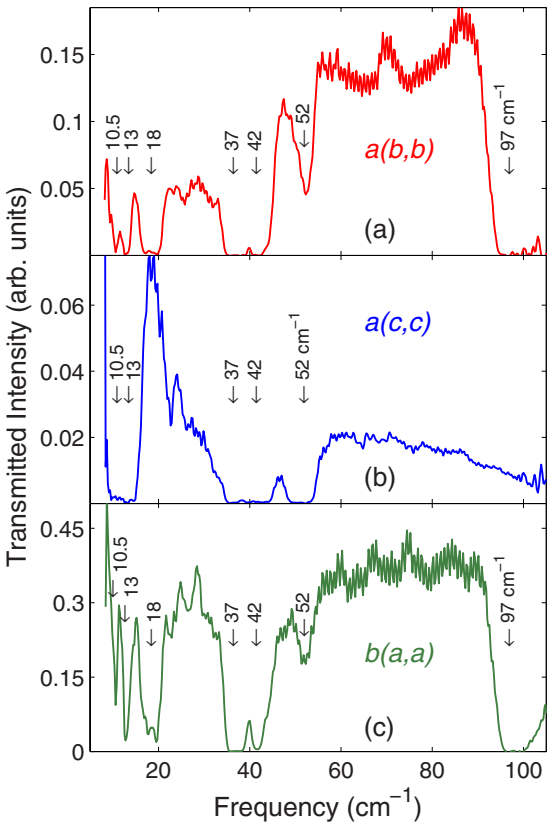

FIG. 1. (Color online) [(a)–(c)] Normalized Fourier-transform far-IR transmission spectra of $HoMn_2O_5$ single crystal measured at $T=5$ K in $a(b,b)$, $a(c,c)$, and $b(a,a)$ configurations, respectively. Arrows indicate the frequencies of IR-active absorption lines.

=150 K. The 18 cm^{-1} oscillator is stronger in $a(b,b)$, is weaker in $b(a,a)$ configurations, and is not optically active for $a(c,c)$ transmission in the entire temperature range. Higher-frequency IR absorption lines do not show significant changes at the phase-transition temperatures. The broad feature at 97 cm^{-1} is polarized in the a-b plane and is not active for the light polarization along c axis in the broad temperature range. Weaker high-frequency absorption peaks at 80 and 85 cm^{-1} develop at the temperatures lower than the commensurate-incommensurate transition T_3, with their oscillator strength increasing quasilinearly with temperature up to about 60 K. Although their strength is small compared to that of other oscillators, these particular high-frequency lines will be important for our interpretation of the observed IR transitions as due to the LF states of Ho^{3+}.

Assignment of the observed IR excitations to electric-dipole or magnetic-dipole transitions is not straightforward in transmission experiments. Additional complication arises in multiferroic crystals due to a possible mixture of magnetic and electric activities for some excitations. In theory, such excitations can contribute to both electric $\chi_e(\omega)$ and magnetic $\chi_m(\omega)$ susceptibilities, both of which are the complex functions of frequency. Thus, a single response function of the sample (e.g., transmission) cannot be used to distinguish between the magnetic- or electric-dipole activity. Among more reliable experimental techniques are variable-incidence-angle reflectivity and, of course, full Muller matrix

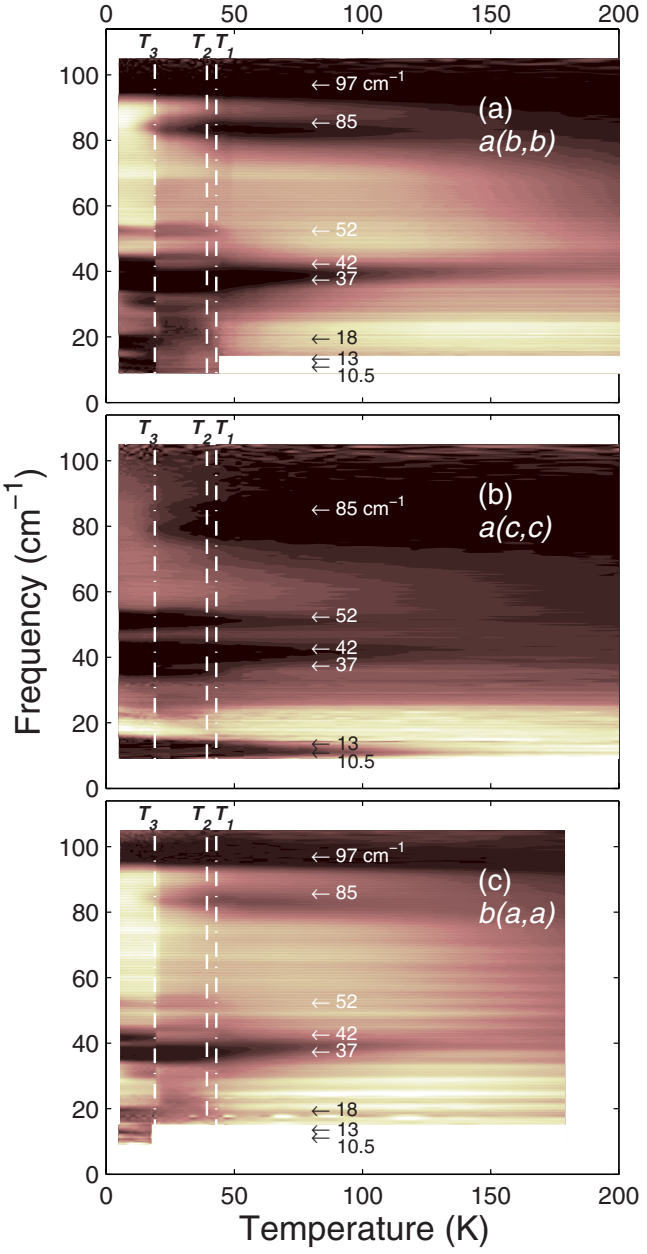

FIG. 2. (Color online) Maps of transmitted intensity vs temperature and frequency for $HoMn_2O_5$ in (a) $a(b,b)$, (b) $a(c,c)$, and (c) $b(a,a)$ configurations. Dark color corresponds to stronger absorption and light color indicates high transmission. The scales of the transmission intensity for each plot are the same as that for the corresponding graphs in Fig. 1.

ellipsometry.[11] Note, however, that these optical techniques are not routinely available due to several factors, such as the lack of broadband quarter-wave plates for the far-IR spectral range and the small size of multiferroic single crystals. Here we will make an attempt to determine the dominating type of the dipole activity for observed IR excitations based on analysis of linear polarization of the transmitted intensity. The main indication of the electric-dipole activity is the domination in only one polarization, like that for the doublet at 10.5 and 13 cm^{-1} in both $a(c,c)$ and $b(c,c)$ configurations. In contrast, the peak at 97 cm^{-1}, which is strong in both $c(a,a)$ *and* $c(b,b)$ and is practically absent in $a(c,c)$ configuration, corresponds to a magnetic dipole polarized along c axis. Table I presents the summary for the frequency, polarization, and dipole activity for the observed IR excitations.

The low-frequency parts of the transmission spectra, which are dominated by the electric-dipole excitations, were fitted using SCOUT-2 software based on the Lorentz model for the parametric description of the dielectric function

$$\varepsilon(\omega) = \varepsilon_\infty + \sum_j^N \frac{S_j \Omega_j^2}{\Omega_j^2 - \omega^2 - i\gamma_j \omega}, \tag{1}$$

where Ω_j, S_j, and γ_j are the oscillator frequency, strength, and damping, respectively. Oscillator parameters for the primary absorption lines are summarized in Table I. Since the oscillator frequencies (Ω_j) are practically constant for all excitations in the temperature range $T \leq 70$ K, it is convenient to present the oscillator strength (S_j) in the same units as that for the static dielectric function by adding Ω_j^2 in the numerator of Eq. (1). The primary changes in the IR spectra at the magnetic phase transitions revealed themselves as an increase in the oscillator strengths but not as the frequency softening, as what is usually observed in ferroelectrics due to the Lyddane-Sachs-Teller relation.[12] Figure 3 shows a comparison between the static dielectric function $[\varepsilon(T)]$ and oscillator strengths $[S_j(T)]$ for electric-dipole active excitations. We can quantitatively relate the steplike behavior of the b-directional static dielectric function $\varepsilon_b(T)$ at T_3 with the contribution of these particular excitations [see Fig. 3(a) and Refs. 2 and 4 for details of dielectric measurements]. In $a(b,b)$ polarization, the low-frequency doublet at 10.5 and 13 cm^{-1} provides the strongest contribution of about 2.2 to $\varepsilon_b(T)$ [Fig. 3(a)]. The 18 cm^{-1} oscillator contributes only about 0.5 at $T < T_3$, which significantly weakens at T_2, and disappears above T_1. The difference in the temperature of the incommensurate-commensurate T_3 transition obtained from IR and dielectric measurements [compare Figs. 3(a) and 3(d)] is due to the thermal hysteresis. Our IR transmission spectra were measured in the warming regime, while dielectric data were taken upon relatively fast cooling. The quantitative discrepancy between $\Delta\varepsilon(T)$ and $\Sigma S_j(T)$ at T_3 can be influenced by systematic errors of experiment, such as oscillator overdamping due to the sample thickness and imperfections of linear polarizers. Note that the magnitude of ε_∞ in the parent compound of $TbMn_2O_5$ has been recently related to the contribution of transverse optical phonons,[7] which should be the case for our $HoMn_2O_5$ crystals as well.

Figure 4 shows temperature dependence for the frequency of IR excitations. No strong variations that exceeded the experimental accuracy of the frequency measurement have been detected at the phase transitions. A natural softening of the 97 cm^{-1} excitation is detected at high temperatures possibly due to interaction with low-frequency optical phonons. Figure 5 represents schematics for most of the observed optical excitations. Temperature-independent excitation frequencies (for $T \leq 70$ K) are represented with horizontal lines. Dashed, dash-dot, and solid lines correspond to the light polarization along a, b, and c directions, respectively.

TABLE I. Polarization, frequency (Ω_j), and oscillator strength (S_j) of the low-frequency ligand-field optical transitions in $HoMn_2O_5$. The units of the oscillator strength (S_j) are the same as that for the static dielectric function. The type of electric dipole, magnetic dipole, or mixed activity is marked with ED, MD, and ED+MD, respectively.

	Polarization	Ω (cm^{-1})	$\langle S_j \rangle$ (T=5–19 K)	Type	Comments
$HoMn_2O_5$	$a(b,b)$	10.5 and 13	1.3	ED	Disappears above T_3
		18	0.6	ED+MD	Disappears above T_2
		37		ED+MD	Disappears above 200 K
		42		ED+MD	Weak, disappears above T_3
		97		MD	
	$b(a,a)$	10.5 and 13	0.5	ED	Disappears above T_3
		18	0.3	ED+MD	Disappears above T_3
		37		ED+MD	Disappears above 150 K
		97		MD	
	$a(c,c)$ and $b(c,c)$	10.5 and 13	3	ED	Disappears above 150 K
		37		ED+MD	Disappears above T_2
		42		ED+MD	Disappears above 150 K
		52		ED	Weak
$TbMn_2O_5$ (Ref. 10)	$\vec{e} \parallel b$	9.6	3.6	ED	Electromagnon (Ref. 10)

All observed IR excitations (except the one at 18 cm^{-1}) remain optically active in at least one polarization configuration in the paramagnetic phase, i.e., at the temperatures well above $T_1 \approx 43$ K (see Fig. 4). Analysis of the results shown in Fig. 5 is given in Sec. III.

III. DISCUSSION

Ho^{3+} in $HoMn_2O_5$ has ten $4f$ electrons. According to Hund's rule, the ground-state term for these ten electrons is ${}^5I_8$.[13] In $HoMn_2O_5$ crystals, 17 states with $J=8$ for Ho $4f$

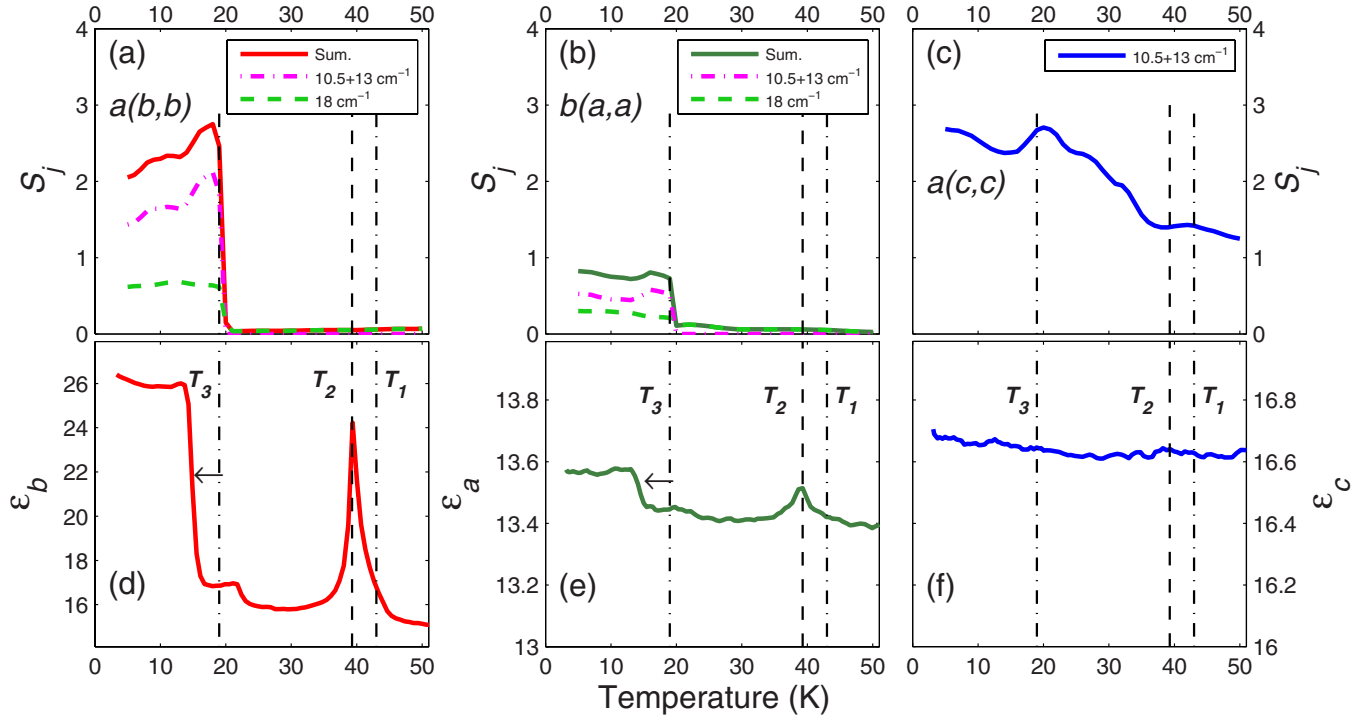

FIG. 3. (Color online) [(a)–(c)] Temperature dependence of the oscillator strength S_j presented in units of the static dielectric function $\varepsilon(0)$ in $a(b,b)$, $b(a,a)$, and $a(c,c)$ polarization configurations, respectively. [(d)–(f)] Temperature dependencies of ε_a, ε_b, and ε_c measured for different orientations of the same $HoMn_2O_5$ crystals. The shift of the T_3 transition temperature between the IR and dielectric measurements is shown with horizontal arrows in (d) and (e).

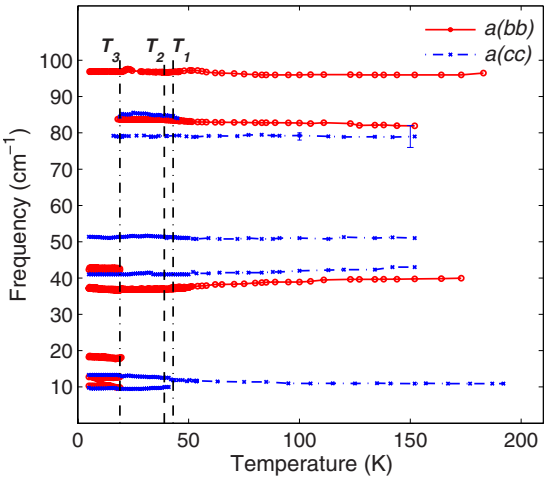

FIG. 4. (Color online) Temperature dependence for the IR oscillator frequencies measured in two polarizations: $a(b,b)$ and $a(c,c)$. The error bars for the 80 cm^{-1} absorption line indicate an increase in the experimental uncertainty at high temperatures.

electrons split due to the ligand field, which, in particular, includes the Hamiltonian term associated with the hybridization of Ho $4f$ and Mn $3d$ orbitals or the covalent bonding term. We distinguish the LF from the crystal field to emphasize that the effect of Mn ions on Ho^{3+} is more complex than the Coulomb potential from point charges. Such hybridization between $4f$ states on Ho^{3+} and $3d$ states on Mn (as occurred, for example, in heavy fermions compounds) is expected to give rise to coupling between spin states of Mn ions and ligand-field states of Ho ions. The role of intervening oxygen ions cannot be neglected in this consideration, and the magnetic interaction between Ho and Mn ions can be considered as the superexchange through the $2p$ orbitals of oxygen.

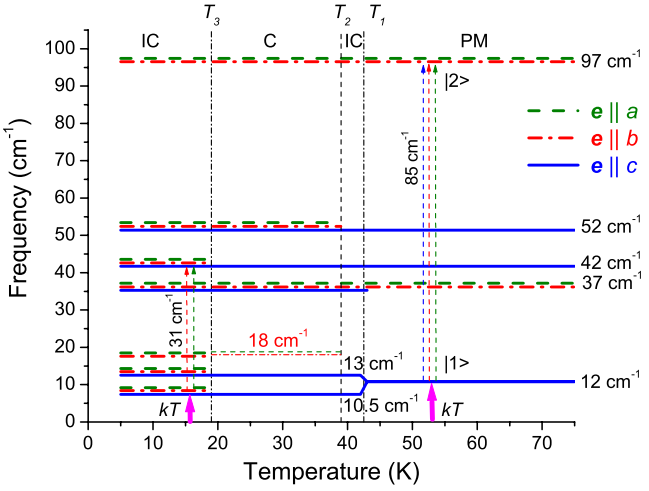

FIG. 5. (Color online) Schematics of the energy diagram for optical transitions between ligand-field split levels of the Ho^{3+} multiplet ($^5I_8$) in $HoMn_2O_5$. The energies of experimentally observed transitions from the ground state are represented with horizontal lines. Dashed, dash-dot, and solid lines indicate the allowed polarization for the corresponding transitions: $a(b,b)$, $b(a,a)$, and $a(c,c)$, respectively. Short vertical arrows indicate thermal activation from the ground state to the nearest excited state with a consecutive optical transition (31 and 85 cm^{-1}) to the higher-energy states. Splitting of the lowest excited state ($12 \rightarrow 10.5+13$ cm^{-1}) occurs in the vicinity of T_2 upon cooling. Vertical dash-dot lines divide different magnetic phases: IC antiferromagnetic (AFM), C AFM, and paramagnetic (PM).

Several neutron-scattering studies of related compounds, such as $HoVO_4$ and $HoMnO_3$, provide us with an estimate for the frequency range of the LF transitions to be between 12 and 300 cm^{-1}.[14,15] For example, the low-energy dispersionless excitations, which have been attributed to the crystal-field splitting of Ho^{3+} in $HoMnO_3$, are at 12 and 25 cm^{-1}. Therefore, we believe that the IR excitations observed in this work for the frequency range up to 100 cm^{-1} in $HoMn_2O_5$ are mostly, with some possible exceptions, dipolar transitions between the ground and the low-energy excited LF states within the $J=8$ multiplets.

For electrons in a centrosymmetric potential, electric-dipole optical transitions between the levels of the $4f^n$ configuration are all forbidden by the parity rule. In contrast, magnetic-dipole transitions are allowed between states of the same parity. The standard angular-momentum method (free ion, LS coupling) gives the selection rules for magnetic-dipole transitions, which are independent of the crystal field. Magnetic dipoles are active between states with $\Delta J=0, \pm 1$, where $\Delta J= \pm 1$ corresponds to transitions between the neighboring multiplet components with $\Delta S=0$, $\Delta L=0$, and $\Delta J=0$ and is meaningful in external magnetic field only. Although this is always true for a free ion, the lower symmetry of the LF potential in crystals can result in appearance of forced electric-dipole transitions in addition to the magnetic-dipole transitions. A forced electric-dipole transition occurs when Ho^{3+} is placed in a LF that has no center of symmetry, such as in RMn_2O_5.[16,17] Hence, the wave function of Ho^{3+} has a mixed parity. The oscillator strength for the forced electric-dipole transition is determined by the admixture of the states with the opposite parity (e.g., d electrons) to the predominantly even parity of Ho^{3+} in the $4f$ (Ref. 10) configuration. Selection rules for the forced electric-dipole transitions depend on the exact symmetry of the LF, and their analysis at the phase transitions in RMn_2O_5 requires separate theoretical studies. Here we will only mention that the selection rules for the forced electric-dipole transitions with $\Delta J=0, \pm 1$ require reversed light polarization (circular σ versus linear π) compared to that for the corresponding magnetic dipoles.[17,18]

According to the Wigner-Eckart theorem,[19] the z-direction dipolar transition between two LF states can be nonzero only if the two states have common J_z components. Similarly, the x- or y-directional dipolar transitions can be nonzero only if the two states have J_z components that are different by ± 1. For $HoMn_2O_5$, we choose the z axis to be parallel to the crystalline c axis. Correspondingly, x and y axes are along crystalline a and b directions. Figure 2 shows that the main change at the magnetic ordering temperatures occurs to the polarization of LF transitions. For instance, the IR excitations at 10.5 and 13 cm^{-1} are present only for the incident light polarized along c direction and are absent for the incident light polarized along a and b directions for the temperature range above T_3. This means that the ground and the excited states at 10.5 and 13 cm^{-1} share the same J_z compo-

nents but do not have any J_z components separated by ± 1 that do not cancel the contribution of each other to the dipole transition matrix element. The appearance of IR excitations at 10.5 and 13 cm^{-1} polarized along a and b axes below T_3 can be interpreted as the symmetry change in either the ground or the excited state in such a way that the ground and the excited states have uncompensated J_z components separated by ± 1. Such changes can occur, for example, through the mixing with another low-energy state, which can be excited from the ground state by a and b polarizations above T_3, such as the one at 37 cm^{-1}.

Modification in the ligand field, which causes such mixing of electron states below T_3, coincides with the commensurate-to-incommensurate AFM phase transition for Mn spins. Since the primary cause of the Ho^{3+} LF splitting is still the electrostatic potential from the surrounding ions, i.e., the crystal-field effect, the *energy* spectrum of the LF states is determined by the electrostatic interaction within the crystal lattice. This energy scale stays practically unchanged in a wide temperature range. However, magnetic effects at $T < T_1$, which appear due to the mixing (or covalent bonding) of Ho^{3+} $4f$ states with the ordered spins of the nearest-neighbor Mn $3d$ states, influence the *symmetry* of LF states, which can change at each magnetic ordering temperature, resulting in transformation of the selection rules for the corresponding optical transitions. The weak nature of $4f$-$3d$ mixing does not allow significant shifts of the level energy (see Fig. 4) but affects, in the first order of the perturbation theory, the *selection rules* for optical transitions. Thus, our results imply that one of the main causes of the sudden steps in the dielectric constant along a and b directions at T_3 can be attributed to the contribution of the forced electric-dipole transitions between the Ho^{3+} LF states due to their coupling to the Mn sublattice. Similar energy scale between magnetic interaction and LF splitting supports the importance of the LF splitting connecting magnetism and dielectric properties of the multiferroic $HoMn_2O_5$ and, probably, of other related RMn_2O_5 compounds with R=Tb and Dy.

In addition to the coupling between R^{3+} LF states and the magnetism on the Mn sublattice, of special interest are the symmetry changes due to magnetically induced lattice modulation and dynamic interactions with the lattice. The latter is especially important for the case when the high-energy LF states are in resonance with the lower-frequency IR-active TO phonons ($\sim$150 cm^{-1}) but this mechanism should not have any strong temperature dependence. In contrast, the influence of magnetostriction on the change in selection rules for the LF transitions can result in anomalies at the phase transitions. However, the strongest changes in the lattice distortion for RMn_2O_5 compounds are usually observed between T_3 and T_1.[20] Since in our experiments the change in selection rules for the LF transitions occurs for $T < T_3$, we consider this as a supporting argument for our interpretation based on the coupling between the magnetism on the Mn sublattice and Ho^{3+} LF states. The splitting of the 12 cm^{-1} state into a doublet (10.5 and 13 cm^{-1}) at $T_C = T_2 = 39$ K can be attributed to the symmetry lowering, which is caused by electric polarization.

The coupling between Mn spin and Ho^{3+} LF state opens the possibility of composite excitations of magnon and LF states in this compound, which are particularly due to their similar energy scale. Two main criteria of identification of such composite excitations should be (i) their activity only in the temperature range below T_1 and (ii) a nonzero dispersion, which is typical for AFM magnons. Can we identify such excitations in our spectra for $HoMn_2O_5$? The only candidate for the composite LF magnon is the peak at 18 cm^{-1}, which is close to the LF transitions at 10.5 and 13 cm^{-1}. This peak dominates in the (b,b) polarization below T_3, maintains sufficient strength above T_3, but is absent for all polarizations above T_1, thus, satisfying the first criterion for electric-dipole active LF-magnon excitations. But since the second criterion cannot be verified with the IR transmission technique, our interpretation requires additional experimental proofs, which can be obtained, for example, using neutron scattering. Thus, the question whether the IR transition at 18 cm^{-1} is a composite LF-magnon excitation or just another LF state, which became electric-dipole active due to the symmetry change below T_1, remains open. In any case, however, we emphasize that the oscillator strength of the excitation at 18 cm^{-1} is only 20% of the combined oscillator strength for the low-frequency LF doublet at 10.5 and 13 cm^{-1}, thus, making this proposed LF magnon to be of secondary importance for explanation of the steplike behavior of the static dielectric function. Appearance of this excitation in (a,a) polarization with a significantly lower oscillator strength can be interpreted as due to a mixed electric- and magnetic-dipole activities of this excitation.

We can also identify excitations from thermally excited LF states (31, 80, and 85 cm^{-1}). The temperature-activated transitions at 31 and 85 cm^{-1} are marked with arrows in Fig. 6(a), which compare two transmission spectra measured at T=5 and 18 K. The absorption peak at 85 cm^{-1} appears below T_3 and becomes stronger as the temperature increases. This IR excitation can be considered as the optical transition from the lowest excited LF state (the doublet at 10.5 and 13 cm^{-1}) to the higher-energy LF state at 97 cm^{-1}. Similarly, the 31 cm^{-1} excitation below T_3 can be considered as the excitation from the same thermally excited LF state to the 42 cm^{-1} excited state. These thermally excited excitations can be found in the temperature-frequency maps in Fig. 2(a), and they are also indicated in Fig. 5 with dashed vertical arrows. For the thermally activated transitions between two excited LF states, $|1\rangle$ and $|2\rangle$, one can expect that the transition probability $W_{|1\rangle\rightarrow|2\rangle}$ depends on temperature-activated occupation of the $|1\rangle$ excited state. At low temperatures, this dependence is dominated by the quasilinear in T term, while at higher temperatures (above 60 K for 85 cm^{-1} transition), depopulation of the ground state to other excited states results in a slow decrease in transition probability. Figure 6(b) compares the probability of the thermally activated transitions $W_{|1\rangle\rightarrow|2\rangle}(T)$, which has been calculated in a simplified six-level model, with experimental data for the oscillator strength of 85 cm^{-1} excitation. Exact calculations should take into account the position and wave-function symmetry for all $4f$ Ho^{3+} states, which should give a better agreement with experiment.

Our IR transmission spectra did not reveal any sharp variations at $T_C = T_2$, and we cannot assign any specific oscillator that changes its strength or frequency, explaining the

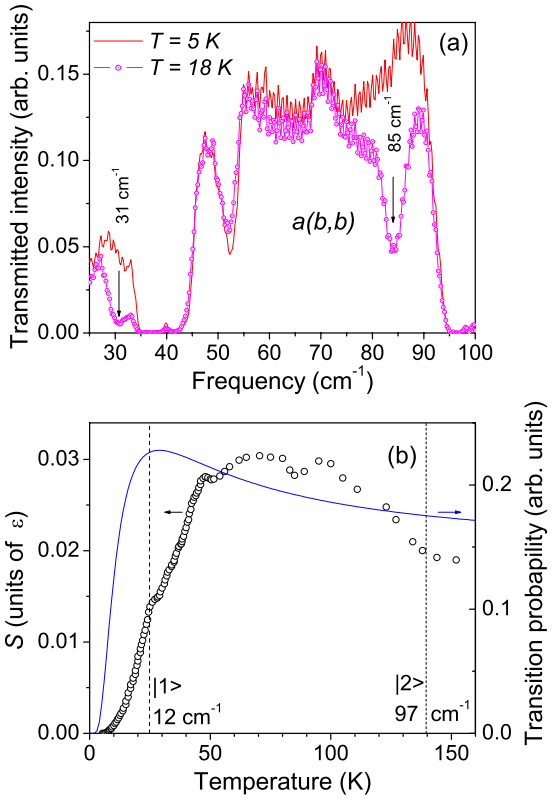

FIG. 6. (Color online) (a) Normalized Fourier-transform far-IR transmission spectra of a $HoMn_2O_5$ single crystal measured at $T=5$ and 18 K in $a(b,b)$ configurations. Arrows indicate the frequencies of the temperature-activated optical transitions at 31 and 85 cm^{-1}. (b) Temperature dependence of the oscillator strength for 85 cm^{-1} transition (circles). Solid curve (right scale) shows the expected trend for the probability of the temperature-activated transition between two excited LF states, $|1\rangle$ at 12 and $|2\rangle$ at 97 cm^{-1}, which was calculated in a simplified model for a six-level system.

spike in $\varepsilon(T)$ at T_2 as shown in Figs. 3(d) and 3(e). The corresponding feature of the static dielectric function in $TbMn_2O_5$ was explained in Ref. 10 by the zero-frequency electromagnon mode. Here we suggest that this peak is related to the spontaneous electric polarization due to the ferroelectric domain structure.

Far-IR transmission spectra in RMn_2O_5 compounds vary for different elements, such as Tb, Dy, and Ho. Both the lowest IR transition frequency and the higher-frequency absorption peaks change for different compounds by a few cm^{-1}. Table I includes frequencies of LF transitions in $HoMn_2O_5$ along with the lowest optical transition frequency in $TbMn_2O_5$, which was attributed to an electromagnon in Ref 10. In contrast to the transmission results for $TbMn_2O_5$ with a strong electromagnon mode at 9.6 cm^{-1} polarized along b axis, in $HoMn_2O_5$ we have observed a LF doublet at 10.5 and 13 cm^{-1}. As was described above, this transition is IR active in both $a(c,c)$ and $a(b,b)$ configurations that are preferably polarized *perpendicular* to the direction of spontaneous polarization b with the polarization degree of $(S^{a(c,c)}-S^{a(b,b)})/(S^{a(c,c)}+S^{a(b,b)})=0.4$. Here $S^{a(c,c)}$ and $S^{a(b,b)}$ are the oscillator strengths from Table I for $a(c,c)$ and $a(b,b)$ configurations, respectively.

We further comment on electromagnon, which is a new composite excitation recently proposed for $RMnO_3$ (R=Gd and Tb) (Ref. 8) and RMn_2O_5 (R=Y and Tb).[10] The origin of electric-dipole activity for this excitation with a typical frequency between 10 and 20 cm^{-1} was attributed in Refs. 9 and 10 to the interaction with optical phonons. In spite of the strong spin-lattice coupling in these multiferroic compounds, it is still under debate whether the two excitations, separated by a large energy scale (optical phonon having usually one order of magnitude larger energy than electromagnons), could experience a direct coupling, which is strong enough to explain magnetoelectric effect. In compounds such as RMn_2O_5 and $RMnO_3$ with R=Gd, Tb, Dy, and Ho (rare-earth ions with f electrons), it might be more fruitful to consider composite excitations between magnons and forced electric-dipole LF excitations since they have a more comparable energy scales. In a general case, dynamic interactions between the lattice and magnons can be mediated by the LF states, which have resonances in both magnon and phonon spectral ranges. For other multiferroic compounds with rare-earth ions without nominal f electrons, the physics can be even more versatile and the concept of electromagnons could be more valuable, especially in the case of YMn_2O_5 compound[10] with a direct $3d$-$3d$ interaction.

IV. CONCLUSIONS

Our experiments demonstrated a strong influence of the ligand field between Ho^{3+} and Mn spin states on IR transmission properties of $HoMn_2O_5$. This coupling can explain the steplike anomalies in the dielectric constant in RMn_2O_5 compounds with rare-earth ions having incomplete $4f$ shell. Further magneto-optical and neutron spectroscopy experiments are required to confirm the existence of LF-magnon composite excitations.

ACKNOWLEDGMENTS

The authors are thankful to C. Bernhard, Dennis Drew, V. Kiryukhin, L. Mihály, and T. Zhou for valuable discussions and to R. Smith for help at U12IR beamline. Work at NJIT was supported by the NSF under Grant No. DMR-0546985. Work at Rutgers was supported by the NSF under Grant No. DMR-0405682. Use of the National Synchrotron Light Source, Brookhaven National Laboratory was supported by the Office of Science, Office of Basic Energy Sciences, U.S. Department of Energy under Contract No. DE-AC02-98CH10886.

*sirenko@njit.edu

[1] N. Hur, S. Park, P. A. Sharma, J. S. Ahn, S. Guha, and S-W. Cheong, Nature (London) **429**, 392 (2004).
[2] C. R. de la Cruz, F. Yen, B. Lorenz, M. M. Gospodinov, C. W. Chu, W. Ratcliff, J. W. Lynn, S. Park, and S. W. Cheong, Phys. Rev. B **73**, 100406(R) (2006).
[3] S-W. Cheong and M. Mostovoy, Nature Mater. **6**, 13 (2007).
[4] C. R. de la Cruz, F. Yen, B. Lorenz, S. Park, S-W. Cheong, M. M. Gospodinov, W. Ratcliff, J. W. Linn, and C. W. Chu, J. Appl. Phys. **99**, 08R103 (2006).
[5] B. Mihailova, M. M. Gospodinov, B. Güttler, F. Yen, A. P. Litvinchuk, and M. N. Iliev, Phys. Rev. B **71**, 172301 (2005).
[6] A. F. García-Flores, E. Granado, H. Martinho, R. R. Urbano, C. Rettori, E. I. Golovenchits, V. A. Sanina, S. B. Oseroff, S. Park, and S.-W. Cheong, Phys. Rev. B **73**, 104411 (2006).
[7] R. Valdés Aguilar, A. B. Sushkov, S. Park, S-W. Cheong, and H. D. Drew, Phys. Rev. B **74**, 184404 (2006).
[8] A. Pimenov, A. A. Mukhin, V. Y. Ivanov, V. D. Travkin, A. M. Balbashov, and A. Loidl, Nat. Phys. **2**, 97 (2006).
[9] H. Katsura, A. V. Balatsky, and N. Nagaosa, Phys. Rev. Lett. **98**, 027203 (2007).
[10] A. B. Sushkov, R. V. Aguilar, S. Park, S-W. Cheong, and H. D. Drew, Phys. Rev. Lett. **98**, 027202 (2007).
[11] R. M. A. Azzam, K. A. Giardina, and A. G. Lopez, Opt. Eng. **30**, 1583 (1991).
[12] A. A. Sirenko, C. Bernhard, A. Golnik, A. M. Clark, J. Hao, W. Si, and X. X. Xi, Nature (London) **404**, 373 (2000).
[13] N. W. Ashcroft, *Solid State Physics* (Holt, Rinehart and Winston, New York, 1976).
[14] S. Skanthakumar, C.-K. Loong, L. Soderholm, M. M. Abraham, and L. A. Boatner, Phys. Rev. B **51**, 12451 (1995).
[15] O. P. Vajk, M. Kenzelmann, J. W. Lynn, S. B. Kim, and S-W. Cheong, Phys. Rev. Lett. **94**, 087601 (2005).
[16] G. R. Blake, L. C. Chapon, P. G. Radaelli, S. Park, N. Hur, S-W. Cheong, and J. Rodríguez-Carvajal, Phys. Rev. B **71**, 214402 (2005).
[17] G. H. Dieke, *Spectra and Energy Levels of Rare Earth Ions in Crystals* (Wiley, New York, 1968).
[18] J. E. Lowther, J. Phys. C **7**, 4393 (1974).
[19] J. J. Sakurai and R. L. Liboff, Am. J. Phys. **54**, 668 (1986).
[20] J. Koo, C. Song, S. Ji, J.-S. Lee, J. Park, T.-H. Jang, C.-H. Yang, J.-H. Park, Y. H. Jeong, K.-B. Lee, T. Y. Koo, Y. J. Park, J.-Y. Kim, D. Wermeille, A. I. Goldman, G. Srajer, S. Park, and S-W. Cheong, Phys. Rev. Lett. **99**, 197601 (2007).